

# Measurements of Fission Product Yield in the Neutron-induced Fission of $^{238}\text{U}$ with Average Energies of 9.35 MeV and 12.52 MeV

Sadhana MUKERJI and Pritam Das KRISHNANI

*Reactor Physics Design Division, Bhabha Atomic Research Centre, Mumbai-400 085, India*

Byrapura Siddaramaiah SHIVASHANKAR

*Department of Statistics, Manipal University, Manipal - 576 104, India*

Vikas Kaluram MULIK

*Department of Physics, University of Pune, Pune - 411007, India*

Saraswatula Venkat SURYANARAYANA

*Nuclear Physics Division, Bhabha Atomic Research Centre, Mumbai -400 085, India*

Haladhara NAIK\* and Ashok GOSWAMI

*Radiochemistry Division, Bhabha Atomic Research Centre, Mumbai -400 085, India*

(Received 7 February 2014, in final form 31 March 2014)

The yields of various fission products in the neutron-induced fission of  $^{238}\text{U}$  with the flux-weighted-averaged neutron energies of 9.35 MeV and 12.52 MeV were determined by using an off-line gamma-ray spectroscopic technique. The neutrons were generated using the  $^7\text{Li}(p, n)$  reaction at Bhabha Atomic Research Centre-Tata Institute of Fundamental Research Pelletron facility, Mumbai. The gamma-ray activities of the fission products were counted in a highly-shielded HPGe detector over a period of several weeks to identify the decaying fission products. At both the neutron energies, the fission-yield values are reported for twelve fission product. The results obtained from the present work have been compared with the similar data for mono-energetic neutrons of comparable energy from the literature and are found to be in good agreement. The peak-to-valley (P/V) ratios were calculated from the fission-yield data and were found to decrease for neutron energy from 9.35 to 12.52 MeV, which indicates the role of excitation energy. The effect of the nuclear structure on the fission product-yield is discussed.

PACS numbers: 25.85.Ec

Keywords: Neutron-induced fission of  $^{238}\text{U}$ , Average neutron energies of 9.35 and 12.52 MeV, Fission products-yield, Off-line gamma-ray spectrometric technique

DOI: 10.3938/jkps.65.18

## I. INTRODUCTION

Nuclear data such as neutron capture cross-sections, fission cross-sections, fission yields and decay data including half-lives, decay energies, branching ratios, etc. are required for many reactor calculations. Among these, the yields of fission products are important from the following reasons: Fission products yields at any time give an idea of the burn-up of the spent fuel. Yields of a few long-lived fission products such as  $^{134}\text{Cs}$ ,  $^{137}\text{Cs}$  and  $^{147}\text{Nd}$  give an idea of the SNF (spent nuclear fuel). Many of the stable nuclides, such as  $^{147}\text{Sm}$ ,  $^{149}\text{Sm}$ ,  $^{151}\text{Eu}$ , and

$^{155}\text{Gd}$ , which contribute to the reactivity of the fuel, are strong absorbers of neutrons. Some of the fission products, which contribute to the radioactivity of the spent nuclear fuel, are  $^{90}\text{Sr}$ ,  $^{90}\text{Y}$ ,  $^{93}\text{Zr}$ ,  $^{99}\text{Tc}$ ,  $^{107}\text{Pd}$ ,  $^{126}\text{Sn}$ ,  $^{129}\text{I}$ ,  $^{135}\text{Cs}$  and  $^{137}\text{Cs}$ . These fission products are unstable and highly radioactive. Some other long-lived fission products have high solubility in water. Hence, there is a risk of migration of these elements if ground water is entering the repository. The yields of short-lived fission products and the independent yields of various fission products in the neutron-induced fission of actinides are important for decay heat calculations [1]. Thus, the yields of fission products contribute towards the design, safety and operation of the nuclear reactors. The calculation of de-

\*E-mail: naikhbar@yahoo.com

cay heat especially within the time of 1 to 1000 seconds after a loss-of-coolant accident is important in a nuclear power plant. The yields of fission products are also used in the calculation of the delayed neutron fraction in reactor fuel, the isotopic composition of nuclear spent fuel and waste inventories. In the case of an accident, the release of fission products to the environment can be estimated from their yields.

From various evaluations [2–7], fission product yields in the thermal neutron-induced fission of actinides are available in sufficient detail for most data-based systems of conventional reactors. However, the advent and the development of advanced reactors, such as fast reactors [8–12], advanced heavy water reactors (AHWR) [13,14] and accelerator driven sub-critical systems (ADSs) [15–17], have highlighted the need for accurate determination of the fission yields in the fast neutron fission of actinides. The potential benefits of advanced nuclear reactors are many and varied, including improved levels of efficiency in the use of fuel, a reduction in the amount of waste and the ability to recycle at least part of the present reactor waste as energy-producing materials. Among the advanced reactors, the fast reactor is based on  $^{238}\text{U}$ - $^{239}\text{Pu}$  fuel, in which transmutation of the fertile isotope  $^{238}\text{U}$  to the fissile isotope  $^{239}\text{Pu}$  takes place. Fast reactors are designed with a core containing  $\sim 15\%$  fissile plutonium and  $85\%$   $^{238}\text{U}$  (depleted uranium) in the form of mixed oxides or carbides surrounded by a blanket of depleted uranium. The fast reactor has a neutron spectrum from 0.1 keV to 15 MeV; therefore, the production of long-lived minor actinides can be suppressed. For the design of a fast reactor, the yield of fast-neutron-induced fission of  $^{238}\text{U}$  and  $^{239}\text{Pu}$  is very much necessary.

Besides the above application, the yields of fission products in the fast neutron induced fission of  $^{238}\text{U}$  are also needed for mass and charge distribution studies, which can provide valuable information for understanding the nuclear fission process. Fission products yields in the fast-neutron-induced fission of various actinides are available in the EXFOR compilation [18], data on reactors [19,20] and fast mono-energetic [21–31] neutron-induced fission of  $^{238}\text{U}$  are available in literature. In the present work, the yields of various fission products in the neutron-induced fission of  $^{238}\text{U}$  with average energies of 9.35 and 12.52 MeV have been determined using an off-line gamma-ray spectrometric technique. The fission yield data measured in present work have been compared with similar data from mono-energetic neutron-induced fission of  $^{238}\text{U}$  to examine the nuclear structure effect.

## II. EXPERIMENTAL DETAILS

The experiment was carried out using the 14UD Bhabha Atomic Research Centre-Tata Institute of Fundamental Research Pelletron Pelletron facility [32] at Mumbai, India. The neutron beam was obtained from

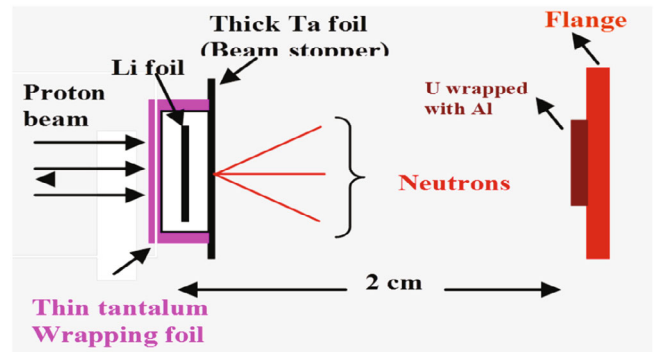


Fig. 1. (Color online) Schematic diagram showing the arrangement used for neutron irradiation

the  $^7\text{Li}(p, n)$  reaction [33,34] by using the main proton beam line at a 6-m height above the analyzing magnet of the Pelletron facility to utilize the maximum proton current from the accelerator. The energy spread for protons at a 6-m height was a maximum of 50 – 90 keV. At this port, the terminal voltage was regulated by using the generated voltage mode (GVM) from the terminal potential stabilizer. Further, we used a collimator of 6 mm diameter before the target. The lithium foil was made up of natural lithium with a thickness of 4.0 mg/cm<sup>2</sup> sandwiched between two tantalum foils of different thicknesses. The front tantalum foil facing the proton beam was the thinnest one, with a thickness of 3.4 mg/cm<sup>2</sup>, in which degradation of the proton energy was only 30 keV [35]. On the other hand, the back tantalum foil was 0.025-mm-thick, which was sufficient to stop the proton beam. Behind the Ta-Li-Ta stack, the sample used for irradiation was natural  $^{238}\text{U}$  metal foils, which were wrapped with 0.025-mm-thick super-pure aluminium foil. The aluminium wrapper was used to stop and collect the fission products recoiling from the surface. The size of the  $^{238}\text{U}$  metal foil was 1.0 cm<sup>2</sup>, and the thickness was 634.2 mg/cm<sup>2</sup>. The  $^{238}\text{U}$  metal foil wrapped with aluminium was mounted at zero degrees with respect to the beam's direction at a distance of 2.1 cm from the location of the Ta-Li-Ta stack. A schematic diagram of the Ta-Li-Ta stack and the  $^{238}\text{U}$  metal foils is shown in Fig. 1. Different sets of samples were made for different irradiations at various neutron energies.

The  $^{238}\text{U}$  metal foils were irradiated for a period of 10 and 5 h with the neutron beams generated by impinging proton beams of 16.0 and 20.0 MeV, respectively on Ta-Li-Ta stack. The proton current during the irradiations varied from 100 to 400 nA. After the irradiation, the samples were cooled for one hour. Then, the irradiated target of  $^{238}\text{U}$ , along with the Al wrapper, was mounted on a Perspex plate and was taken for  $\gamma$ -ray spectrometry. The  $\gamma$ -rays from the fission/reaction products of the irradiated  $^{238}\text{U}$  sample were counted in an energy- and efficiency-calibrated 80-c.c. HPGc detector coupled to a PC-based 4K channel analyzer. The HPGc detector was a p-type co-axial ORTEC detector of 4.5 cm in diame-

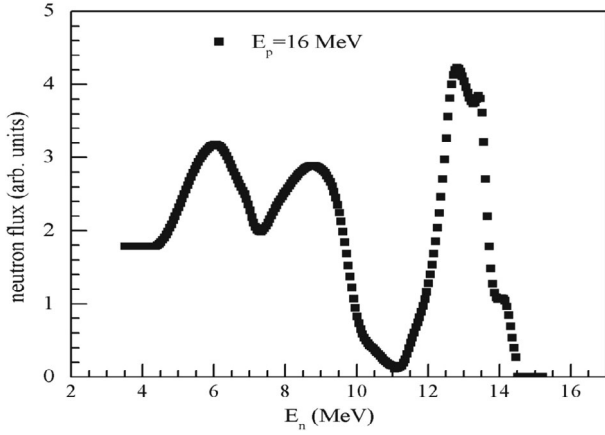


Fig. 2. Neutron spectrum from  ${}^7\text{Li}(p, n)$  reaction at  $E_p = 16.0$  MeV calculated using the results of Meadows and Smith of Ref. [36].

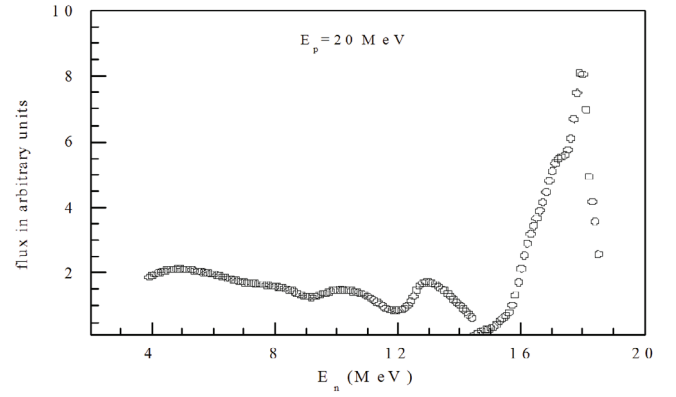


Fig. 3. Neutron spectrum from  ${}^7\text{Li}(p, n)$  reaction at  $E_p = 20.0$  MeV calculated using the results of Meadows and Smith of Ref. [36].

ter and 5 cm in length. The resolution of the detector system had a FWHM of 1.8 keV  $\gamma$ -line at 1332.5-keV of  ${}^{60}\text{Co}$ . The energy- and the efficiency-calibrations of the detector system were done by counting the  $\gamma$ -ray energies from a standard  ${}^{152}\text{Eu}$  source in the same geometry, where the summation error was negligible. This was checked by comparing the efficiency obtained from  $\gamma$ -ray counting of standards such as  ${}^{241}\text{Am}$  (59.54 keV),  ${}^{133}\text{Ba}$  (80.997, 276.4, 302.9, 356.02 & 383.82 keV),  ${}^{137}\text{Cs}$  (661.66 keV),  ${}^{54}\text{Mn}$  (834.55 keV) and  ${}^{60}\text{Co}$  (1173.23 & 1332.5 keV). The detector efficiency was 20% at 1332.5 keV relative to a 3" diameter x 3" length NaI (Tl) detector. The efficiency of the detector system decreased with increasing or decreasing of  $\gamma$ -ray energy above and below 121.8 keV, respectively. The uncertainty in the efficiency was 2 – 3%. The counting dead time was always kept less than 5% by placing the irradiated  ${}^{238}\text{U}$  sample at a suitable distance from the detector to avoid pileup effects. The  $\gamma$ -ray counting of the irradiated  ${}^{238}\text{U}$  sample was done for a few months to check the half-life of the nuclides of interest.

### III. DATA ANALYSIS

#### 1. Calculation of neutron energy

In the present experiment, the incident proton energies were 16.0 MeV and 20.0 MeV. The degradation of the proton energy in the front thin tantalum foil was only 40 – 50 keV [35]. The Q-value for the  ${}^7\text{Li}(p, n){}^7\text{Be}$  reaction to the ground state is  $-1.644$  MeV whereas the first excited state is at 0.431 MeV above the ground state, leading to a Q-value of  $-2.079$  MeV [36–38]. The ground state of  ${}^7\text{Be}$  has a threshold of 1.881 MeV whereas the first excited state of  ${}^7\text{Be}$  has a threshold of 2.38 MeV. With  ${}^7\text{Li}$ , a second neutron group at  $E_p \geq 2.4$  MeV is

produced due to the population of the first excited state of  ${}^7\text{Be}$ . Thus, for the proton energies of 16 MeV and 20 MeV, neutron energies  $n_0$  for the first group will be 14.12 MeV and 18.12 MeV relative to the ground state of  ${}^7\text{Be}$  [36–39]. For the first excited state of  ${}^7\text{Be}$ , the neutron energies of the second group of neutrons ( $n_1$ ) will be 13.62 MeV and 17.62 MeV, respectively. Fragmentation of  ${}^8\text{Be}^*$  to  ${}^4\text{He} + {}^3\text{He} + n$  ( $Q = -3.23$  MeV) also occurs when the proton energy exceeds 4.5 MeV and other reaction channels are open to give a continuous neutron distribution besides the  $n_0$  and the  $n_1$  groups of neutrons. For a proton energies of 16.0 MeV and 20.0 MeV, the neutron spectrum for the  ${}^7\text{Li}(p, n)$  reaction has been generated [33,34] by using the neutron energy distribution given by Meadows and Smith [36]. Typical neutron spectra from the  ${}^7\text{Li}(p, n)$  reaction for proton energies of 16 MeV and 20 MeV are shown in Figs. 2 and 3, respectively. These figures show that the neutron flux changes with neutron energy. Based on the neutron spectra, the flux-weighted average neutron energy ( $\langle E_n \rangle$ ) has been calculated using the following equation:

$$\langle E_n \rangle = \frac{\sum E_n \varphi}{\sum \varphi} \quad (1)$$

where  $\varphi$  is the neutron flux corresponding to the neutron energy  $E_n$ . From Eq. (1), the average neutron energies were obtained as 9.35 MeV and 12.52 MeV for the proton energies of 16 MeV and 20 MeV, respectively.

#### 2. Calculation of Fission Yields

The net photo-peak areas of different  $\gamma$ -rays of interest were calculated by subtracting the linear background from their gross peak areas. The number of  $\gamma$ -rays detected ( $A_{obs}$ ) under the photo-peak of each individual fission products is related to the cumulative yield ( $Y_c$ )

Table 1. Nuclear spectroscopic data and yields of fission products in the neutron induced fission of  $^{238}\text{U}$  at average neutron energy of 9.35 MeV and 11.3 MeV [31], taking yield of  $^{97}\text{Zr}$  (5.206%) as reference for 14 MeV incident neutrons from ref. [41].

Nuclide	Half-life	$\gamma$ -ray		Y(%)	
		Energy (keV)	abundance (%)	Present work	Ref. [31]
$^{91}\text{Sr}$	9.63 h	1024.3	33.0	$3.831 \pm 0.211$	$3.93 \pm 0.15$
$^{92}\text{Sr}$	2.71 h	1384.9	90.0	$3.976 \pm 0.412$	$4.18 \pm 0.14$
$^{95}\text{Zr}$	64.02 d	756.7	54.0	$4.687 \pm 0.121$	$5.18 \pm 0.18$
$^{97}\text{Zr}$	16.91 h	743.4	93.0	$5.206 \pm 0.412$	$5.28 \pm 0.20$
$^{105}\text{Ru}$	4.44 h	724.4	47.0	$3.346 \pm 0.302$	$3.64 \pm 0.18$
$^{115}\text{Cd}^g$	53.46 h	336.2	45.9	$0.541 \pm 0.051$	-
$^{129}\text{Sb}$	4.32 h	812.4	43.0	$1.441 \pm 0.151$	$1.50 \pm 0.094$
$^{132}\text{Te}$	3.2 d	228.1	88.0	$5.184 \pm 0.402$	$5.36 \pm 0.21$
$^{133}\text{I}$	20.8 h	529.9	87.0	$5.301 \pm 0.401$	$6.66 \pm 0.26$
$^{139}\text{Ba}$	83.03 min	165.8	23.7	$4.511 \pm 0.405$	$5.1 \pm 0.30$
$^{143}\text{Ce}$	33.03 h	293.3	42.8	$3.306 \pm 0.351$	$4.28 \pm 0.16$
$^{147}\text{Nd}$	10.98 d	91.1	28.0	$2.209 \pm 0.101$	$2.39 \pm 0.10$

Table 2. Nuclear spectroscopic data and yields of fission products in the neutron induced fission of  $^{238}\text{U}$  at average neutron energies of 12.52 MeV and 14.1 MeV [26], taking yield of  $^{97}\text{Zr}$  (5.206%) as reference for 14.0 MeV incident neutrons from ref. [41].

Nuclide	Half-life	$\gamma$ -ray		Y(%)	
		Energy (keV)	abundance (%)	Present work	Ref. [26]
$^{91}\text{Sr}$	9.63 h	1024.3	33.0	$3.560 \pm 0.151$	$3.59 \pm 0.20$
$^{92}\text{Sr}$	2.71 h	1384.9	90.0	$3.705 \pm 0.351$	$3.87 \pm 0.26$
$^{95}\text{Zr}$	64.02 d	756.7	54.0	$4.950 \pm 0.122$	$4.72 \pm 0.27$
$^{97}\text{Zr}$	16.91 h	743.4	93.0	$5.206 \pm 0.412$	$4.94 \pm 0.32$
$^{105}\text{Ru}$	4.44 h	724.4	47.0	$3.520 \pm 0.404$	$3.64 \pm 0.18$
$^{115}\text{Cd}^g$	53.46 h	336.2	45.9	$1.061 \pm 0.301$	$0.97 \pm 0.15$
$^{129}\text{Sb}$	4.32 h	812.4	43.0	$1.491 \pm 0.205$	$1.56 \pm 0.13$
$^{132}\text{Te}$	3.2 d	228.1	88.0	$4.501 \pm 0.404$	$4.31 \pm 0.24$
$^{133}\text{I}$	20.8 h	529.9	87.0	$5.051 \pm 0.405$	$5.73 \pm 0.37$
$^{139}\text{Ba}$	83.03 min	165.8	23.7	$4.706 \pm 0.406$	$5.10 \pm 0.32$
$^{143}\text{Ce}$	33.03 h	293.3	42.8	$3.110 \pm 0.361$	$3.62 \pm 0.19$
$^{147}\text{Nd}$	10.98 d	91.1	28.0	$2.393 \pm 0.110$	$2.01 \pm 0.14$

as follows

$$A_{obs}(CL/LT) = N\sigma_f(E)\Phi I_\gamma \varepsilon Y_c (1 - e^{-\lambda t}) e^{-\lambda T} (1 - e^{-\lambda LT}) / \lambda \quad (2)$$

where,  $N$  = the number of target atoms,  $\sigma_f(E)$  = the neutron-induced fission cross-section as a function of neutron energy ( $E$ ) of the target with an average neutron flux ( $\Phi$ ),  $I_\gamma$  = the branching intensity for the  $\gamma$ -ray of the fission product,  $\varepsilon$  = the efficiency of the detector system, which changes with gamma ray energy,  $t$  = the irradiation time,  $T_c$  = the cooling time and  $CL$  and  $LT$  = the clock time and the live time of counting, respectively.

The nuclear spectroscopic data, such as the  $\gamma$ -ray en-

ergy, the branching intensity and the half-life of the fission products are taken from Refs. 39 and 40. The cumulative yields of the fission products relative to that of the fission rate monitor  $^{97}\text{Zr}$  were calculated using Eq. (1). The yield of the fission rate monitor  $^{97}\text{Zr}$  was chosen from the point of view of the near constant yield with changing neutron energy [21–31]. For neutron energies of 9.35 MeV and 12.52 MeV, the fission-yield data of  $^{97}\text{Zr}$  in the 14-MeV neutron-induced fission of  $^{238}\text{U}$  was taken from Ref. 41.

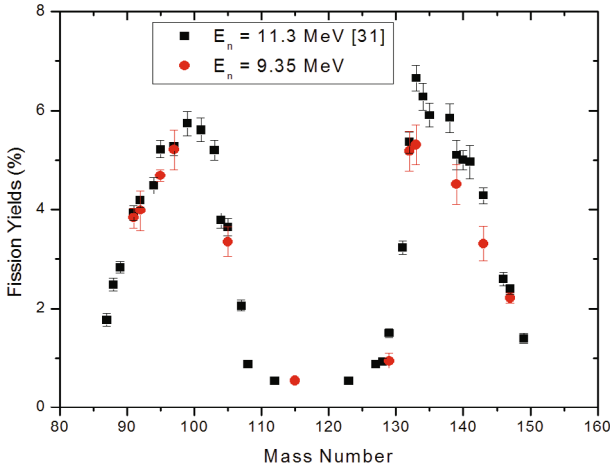


Fig. 4. (Color online) Fission yield of fission products for  $E_n = 9.35$  MeV compared to 11.3 MeV values taken from ref. [31].

#### IV. RESULTS AND DISCUSSION

The cumulative yields of various fission products relative to  $^{97}\text{Zr}$  in the neutron-induced fission of  $^{238}\text{U}$  at flux-weighted average neutron energies of 9.35 and 12.52 MeV, along with nuclear spectroscopic data, are given in Tables 1 and 2, respectively. The uncertainties associated to the measured cumulative yields come from a combination of two experimental data sets with replicate measurements. The overall uncertainty is the quadratic sum of both the statistical and the systematic errors. The random error in the observed activity is particularly due to counting statistics, which is estimated to be 5 – 10%. This was determined by accumulating data for an optimum time period that depended on the half-life of the nuclide of interest. The systematic errors are due to uncertainties in the neutron flux estimate ( $\sim 3\%$ ), the irradiation time ( $\sim 0.5\%$ ), the detector efficiency ( $\sim 3\%$ ) and the half-life of fission products and  $\gamma$ -ray abundances ( $\sim 2\%$ ). The overall uncertainty was in the range of 7 – 11%, coming from a combination of the statistical error of 5 – 10% and the systematic error of 4.7%.

The cumulative yields of different fission products in the present work for the 9.35-MeV and 12.52-MeV neutron-induced fission of  $^{238}\text{U}$  were determined for the first time. The literature data for the mono-energetic neutrons of 11.3 MeV [31] and 14.1 MeV [26] are given in the Tables 1 and 2 to compare with the present data at average neutron energies of 9.35 MeV and 12.52 MeV. From Tables 1 and 2, the cumulative fission yields of the twelve fission products determined in the present work at two different flux-weighted average neutron energies can be seen to be in general agreement with the literature data [26, 31] based on mono-energetic neutron-induced fission of  $^{238}\text{U}$ . The yields of various fission products in the neutron energies of 9.35 MeV and 12.52 MeV from the present work and the literature data for comparable

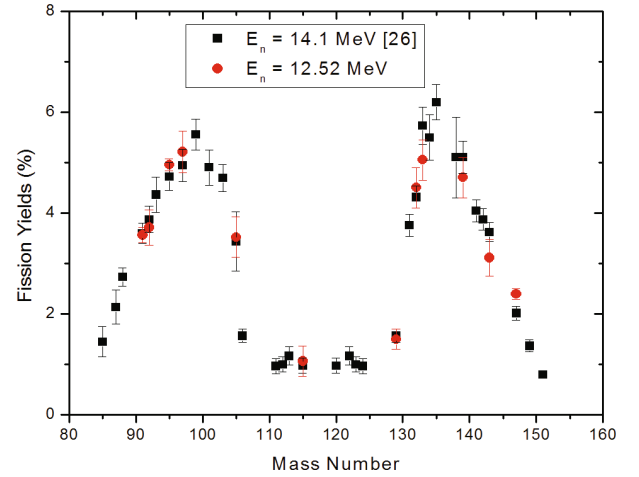


Fig. 5. (Color online) Fission yield of fission products for  $E_n = 12.52$  MeV compared to 14.1 MeV values taken from ref. [26].

neutron energies of 11.3 MeV [31] and 14.1 MeV [26] are also plotted in Figs. 4 and 5, respectively. From Figs. 4 and 5, the fission yield distribution in the 9.35-MeV and 12.52-MeV neutron-induced fission of  $^{238}\text{U}$  can be seen to be double humped. The peak-to-valley ratio was calculated from the fission yield data as the ratio of yields of  $^{133}\text{I}$  to  $^{115g}\text{Cd}$  and was found to be  $9.8 \pm 0.9$  and  $4.8 \pm 1.4$  for neutron energies of 9.35 MeV and 12.52 MeV, respectively. If one considers the peak-yield data (Figs. 4 and 5) from the literature for  $^{133}\text{I}$  ( $6.66 \pm 0.26\%$ ) [31], for  $^{135}\text{Xe}$  ( $6.19 \pm 0.35\%$ ) [26] and the yield of  $^{115g}\text{Cd}$  from Tables 1 and 2, then the peak-to-valley ratios will be  $12.3 \pm 1.6$  at 9.35 MeV and  $5.8 \pm 1.7$  at 12.52 MeV, which are slightly higher than the values in the present work. The peak-to-valley (P/V) ratio at average neutron energy of 12.52 MeV is lower than at 9.35 MeV, which indicates the role of excitation energy.

Figures 4 and 5 also show that the yields of fission products around mass numbers 133 – 134 and their complementary products are higher than the yields of other fission products [19, 20]. The higher yields of the fission products for  $A = 133 - 134$  and  $143 - 144$  can be explained from the point of view of the standard I and standard II asymmetric fission modes, as mentioned by Brossa *et al.* [42], which arise due to shell effects [43]. Based on standard I asymmetry, the fissioning system is characterized by spherical, heavy fragments with mass numbers 133 – 134 due to the spherical  $82n$  shell and a deformed complementary light mass fragment. Based on standard II asymmetry, the fissioning system is characterized by a deformed heavy-mass fragment near mass numbers 143 – 144 due to a deformed  $86 - 88n$  shell and slightly deformed light mass fragment. Thus, the higher yields of the fission products for  $A = 133 - 134$  and  $143 - 144$  are due to the presence of spherical  $82n$  and a deformed  $86 - 88n$  shells, respectively. Besides this, the peaking of fission yields at the mass region 133 – 134,



138 – 139, 143 – 144 and their complementary products corresponding to alternate most probable even- $Z$  52, 54 and 56, nuclei are based on the  $A/Z$  ratio of 2.5, which is comparable to that of the fissioning system. This has been very well observed at lower average neutron energies [19,20], which indicates the role of the even-odd effect in addition to the shell effect. However, in the present case, the higher yield of fission products is well pronounced only for  $A = 133 - 134$  and complementary products but not for  $A = 138 - 139$  and  $A = 143 - 144$  and their complementary products. This indicates that the even-odd effect does not persist or it is very weak at neutron energies of 9.35 MeV and 12.52 MeV. The higher yields of fission products around mass numbers 133 – 134 and complementary product is because of a shell combination of complementary pairs. For fission products with mass numbers 133 – 134, if the neutron emission is about one, then it correspond to the fragment mass of 134 – 135, with the most probable  $52p$  and the spherical  $82n$  shells. Accordingly, the complementary fragment has a mass number of 105 – 104, respectively, corresponding to the most probable  $40p$  and the deformed  $64n$  shells. The fission products of  $A = 143 - 144$  have the most probable  $56p$  and deformed  $88n$  shells. However, complementary products do not have any shells due to the higher number of neutron emissions. Thus, in the 9.35- to 12.52-MeV neutron-induced fission of  $^{238}\text{U}$ , the yields of fission products for  $A = 133 - 134$  and its complementary products, the shell effect is observed very well. However, for fission products with  $A = 143 - 144$  and their complementary products, the shell effect is less pronounced. This indicates that the shell pair combination of complementary products affects the yield profile, even at the high neutron energies of 9.35 MeV and 12.52 MeV. This observation also indicates that the shell effect exists even in the 9.35-MeV and 12.52-MeV neutron-induced fission of  $^{238}\text{U}$ .

## V. CONCLUSION

The yields of twelve fission products in neutron-induced fission of  $^{238}\text{U}$  at average neutron energies of 9.35 and 12.52 MeV were determined for the first time by using an off-line gamma ray spectrometric technique. The present data at average neutron energies of 9.35 and 12.52 MeV are in close agreement with similar data based on mono-energetic neutron induced fission of  $^{238}\text{U}$  at 11.3 and 14.1 MeV, respectively. In addition, the fission product's yield distribution in the neutron induced fission of  $^{238}\text{U}$  at average neutron energies of 9.35 and 12.52 MeV are double humped. However, the peak-to-valley (P/V) ratio decreases with increasing neutron energy from 9.35 to 12.52 MeV. This indicates the role of the excitation energy. Finally, the higher yields of fission products around mass numbers 133 – 134 and their complementary products are due to a combination of the spherical  $82n$  and

the deformed  $62n$  shells. This observation indicates that the effect of nuclear structure persist even at high neutron energies of 9.35 and 12.52 MeV.

## ACKNOWLEDGMENTS

The authors are thankful to the staff of Bhabha Atomic Research Centre-Tata Institute of Fundamental Research Pelletron facility for their kind co-operation and help in providing the proton beam to carry out the experiment. We are also thankful to Mr. Ajit Mahadakar and Mrs. Dipa Thapa from the target laboratory of the Pelletron facility at TIFR, Mumbai, for providing us the Li and Ta targets. One of the author (Sadhana Mukerji) thanks Dr. (Mrs.) Suparna Sodaye of the Radiochemistry Division, BARC, for her cooperation and help in the spectrum analysis of this work.

## REFERENCES

- [1] K. Oyamatsu, H. Takeuchi, M. Sagisaki and J. Katahura, *J. Nucl. Sci. Technol.* **38**, 477 (2001).
- [2] B. F. Rider, *Compilation of Fission Products Yields*, EDO, 12154 3c ENDF-327, Vallecitos Nuclear Centre (1981) (<http://www.nds.iaea.org>).
- [3] T. R. England and B. F. Rider, *Evaluation and Compilation of Fission Products Yields*, ENDF0BVI (1989) (<http://www.nds.iaea.org>).
- [4] M. James and R. Mills, *Neutron Induced Fission Products Yields*, UKFY2 -1991.
- [5] F. Vivès, F. Hamsch, H. Box and S. Oberstedt, *Nucl. Phys. A* **662**, 63 (2000).
- [6] A. Koning, M. Forrest, R. Kellett, H. Henriksson and Y. Rugama, *The JEFF-3.1 Nuclear Data Library*, JEFF Report 21, OECD/NEA, Paris, France, ISBN 92-64-02314-3 (2006).
- [7] D. Gorodisskiy, K. Kovalchuk, S. Mulgin, A. Rusanov and S. Zhdanov, *Ann. Nuc. Energy.* **35**, 238 (2008).
- [8] Fast Reactors and Accelerator Driven Systems Knowledge Base, IAEA-TECDOC-1319: Thorium fuel utilization: Options and Trends, ([https://www.nds.iaea.org/publications/group\\_list.php?group=TECDOCS](https://www.nds.iaea.org/publications/group_list.php?group=TECDOCS)).
- [9] P. E. MacDonald and N. Todreas, ANUAL Project Status Report 2000, MIT-ANP-PR-071, INEFL/EXT-2009-00994 (2000).
- [10] L. Mathieu *et al.*, In *Proceedings of Global International Conference*, (Tsukuba 2005), p. 100.
- [11] A. Nuttin *et al.*, *Proc. Nucl. Energy.* **46**, 77 (2005).
- [12] T. R. Allen and D.C. Crawford, *Science and Technology of Nuclear Installations*, Article ID 97486 (2007).
- [13] R. K. Sinha and A. Kakodkar, *Nucl. Eng. Des.* **236**, 683 (2006).
- [14] S. Ganesan, *Third research coordination meeting*, (30 Jan - 2 Feb 2006, Vienna, INDC), (NDS)- 0494.
- [15] S. Ganesan and Pramana, *Journal of Physics* **68**, 257 (2007).

- [16] F. Carminati, R. Klapisch, J. P. Revol, Ch. Roche, J. A. Rubio and C. Rubbia, CERN Report No. CERN/AT/93-47 (ET), 1993.
- [17] C. Rubbia *et al.*, CERN/AT/95-44 (ET) 1995.
- [18] Joint Evaluated Fission and Fusion File, Incident neutron data, <http://www.nds.iaea.org/exfor/endf00.htm>, 2 October 2006.
- [19] H. Naik, A. G. C. Nair, P. C. Kalsi, A. K. Pandey, R. J. Singh, A. Ramaswami and R. H. Iyer, *Radiochim. Acta.* **75**, 69 (1996).
- [20] R. H. Iyer, H. Naik, A. K. Pandey, P. C. Kalsi, R. J. Singh, A. Ramaswami, A. G. C. Nair, *Nucl. Sci. Eng.* **135**, 227 (2000).
- [21] K. M. Broom, *Phys. Rev.* **126**, 627 (1962).
- [22] N. Borisova, S. M. Dubrovina, V. I. Novgorodtseva, V. A. Pchelina, V. A. Shigin and V. M. Shubko, *Sov. J. Nucl. Phys.* **6**, 331 (1968).
- [23] D. J. Gorman and R. H. Tomilson, *Can. J. Chem.* **46**, 1663 (1968).
- [24] J. T. Harvey, D. E. Adams, W. D. James, J. N. Beck, J. L. Meason and P. K. Kuroda, *J. Inorg. Nucl. Chem.* **37**, 2243 (1975).
- [25] D. E. Adams, W. D. James, J. N. Beck and P. K. Kuroda, *J. Inorg. Nucl. Chem.* **37**, 419 (1975).
- [26] M. Rajagopalan, H. S. Pruyss., A. Grutter, E. A. Hermes and H. R. Von Gunten, *J. Inorg. Nucl. Chem.* **38**, 351 (1976).
- [27] T. C. Chapman, G. A. Anzelon, G. C. Spitale and D. R. Nethaway, *Phys. Rev. C* **17**, 1089 (1978).
- [28] L. Conggui, L. Huijun and L. Yonghui, *High Energy Phys and Nucl Phys (Chinese)* **7**, 235 (1985).
- [29] S. Nagy, K. F. Flynn., J. E. Gindler., J. Meadows and E. Glendenin, *Phys. Rev. C* **17**, 163 (1978).
- [30] A. Afarideh and K. R. Annole, *Ann. Nucl. Energy.* **16**, 313 (1989).
- [31] Z. Li *et al.*, *Radiochim. Acta.* **64**, 95 (1994).
- [32] S. S. Kapoor, V. A. Hattangadi and M. S. Bhatia, *Indian J. Pure and Appl. Phys.* **27**, 623 (1989).
- [33] H. Naik *et al.*, *Eur. Phys. J. A* **47**, 51 (2011).
- [34] S. Mukerji, H. Naik, S. V. Suryanarayana, S. Chachara, B. S. Shivashankar, V. K. Mulik, S. Samanta., A. Goswami and P. D. Krishnani, *J. Basic and App. Phys.* **2**, 104 (2013).
- [35] J. F. Ziegler, M. D. Zeigler and J. P. Biersack, *Nucl. Instr. Meth. B*, **268**, 1818 (2010).
- [36] J. W. Meadows and D. L. Smith, Argonne National Laboratory Report ANL-7983 (1972).
- [37] G. Mashnik, M. B. Chadwick., H. G. Hughes, R. C. Little., R. E. Macfarlane, L. S. Waters and P. G. Young, arXiv: nucl-th/0011066v117, Los Alamos National Laboratory (Nov. 2000).
- [38] C. H. Poppel, J. D. Anderson, J. C. Davis, S. M. Grimes, C Wong, *Phys. Rev. C* **14**, 438 (1976).
- [39] NuDat (BNL, U.S.A), [www.nndc.bnl.gov/nudat2/](http://www.nndc.bnl.gov/nudat2/).
- [40] B. Browne and R. B. Firestone, in *Table of Radioactive Isotopes*, edited by V.S Shirley, (Wiley, New York, 1986); R. B. Firestone and L. P. Ekstrom, in *Table of Radioactive Isotopes*, Version 2.1 (2004) [<http://ie.lbl.gov/toi/index.asp>].
- [41] S. Daroczy, P. Baics and S. Nagy, in *Proceedings of the Panel on Fission Product Nuclear Data*, (see ref. 6) Vol. 3, p. 281.
- [42] U. Brossa, S. Grossmann, A. Muller, *Phys. Rep.* **197**, 167 (1990),
- [43] B. D. Wilkins, E. P. Steinberg and R. R. Chasman, *Phys. Rev. C* **14**, 1832 (1976).